PHYSICAL REVIEW E **73**, 025202(R) (2006)

Wave-vector resonance in a nonlinear multiwavespeed chaotic billiard

Alexei Akolzin and Richard L. Weaver
Department of Theoretical and Applied Mechanics, University of Illinois, 104 South Wright Street, Urbana, Illinois 61801, USA
(Received 9 August 2005; published 15 February 2006)

Nonlinear coupling between eigenmodes of a system leads to spectral energy redistribution. For multiwavespeed chaotic billiards, the average coupling strength can exhibit sharp discontinuities as a function of frequency related to wave-vector coincidences between constituent waves of different wavespeeds. The phenomenon is investigated numerically for an ensemble of two-dimensional square two-wavespeed billiards with rough boundaries and quadratic nonlinearity representative of elastodynamic waves. Results of direct numerical simulations are compared with theoretical predictions.

DOI: 10.1103/PhysRevE.73.025202 PACS number(s): 05.45.Mt, 43.25.+y, 43.35.+d, 62.30.+d

Recent years have been marked by increased attention to multiple scattering and propagation of classical waves in disordered nonlinear media. The main research has been in optics; see [1] and references therein. Characteristics of a wavefield pertinent to continuous-wave problems, such as angular correlations and coherent backscattering, have dominated [2]. The influence of nonlinearity on the stability of a speckle pattern has been considered also [3]; nonlinear phenomena in transient fields, as, for example, frequency shifting of a lasing-mode in a random laser [4], have been studied.

An anisotropic or multiwavespeed nature of the medium supporting propagation of the classical waves allows a broader ground for interplay between nonlinearity and multiple scattering. Statistical effects of nonlinear wave-field behavior have received little attention so far. A class of systems in which these effects are expected is given by elastodynamic waves in solids, with anisotropy or multiple speeds of propagation as a rule rather than exception. Ballistic billiards in the form of elastic solids with a ray-chaotic shape are conveniently realizable and allow ready access to the time domain and observation of transients [5]. These billiards are representative of classical wave-bearing systems, and are suited for the study of statistical nonlinear effects that stem from the multiple-wavespeed character of the wave-field. The purpose of this study is to provide evidence of one such effect, namely wave-vector resonance in a chaotic nonlinear billiard, with an elastodynamic billiard chosen as an underlying physical model. In Ref. [6] it was predicted that the strength of nonlinear coupling among waves of different types undergoes a discontinuity at certain characteristic frequency ratios.

Dynamics of an elastodynamic billiard after excitation by a transient source can be reduced in the absence of energy dissipation to a set of nonlinearly coupled oscillators with natural frequencies ω_k, amplitudes of vibration d_k, and coupling matrices N [6],

$$\ddot{d}_k + \omega_k^2 d_k + N_{klm} d_l d_m + N_{klmn} d_l d_m d_n = 0, \tag{1}$$

where nonlinearity up to cubic terms has been accounted for. Associated with each oscillator (mode) is its linear energy $E_k=(\dot{d}_k^2+\omega_k^2 d_k^2)/2$. Although not being true energy in the presence of nonlinearity, E_k elucidates trends of modal energy redistribution when nonlinearity is weak.

For observation times much smaller than the inverse modal spacing, $t \ll D$, individual modes are not resolved, and statistical description is in order. One of the energy quantities conveniently accessible for experimental measurement under these conditions is the average spectral density, $E(\omega_k,t) = D(\omega_k)\langle E_k(t)\rangle$, a constant in the absence of dissipation or nonlinearity. Under the influence of nonlinearity it evolves in time. The evolution leads to energy deposit into frequencies that contained no energy initially, thereby allowing detection of the nonlinearity. In the case of a weak nonlinearity, the leading contribution to the deposit is given by convolution of energy densities at two frequencies that have a given (target) frequency ω as a combination, i.e., their sum or difference [6],

$$\dot{E}(\omega,t) = D(\omega)\int_0^{+\infty} d\omega' \sum_{\pm} \mathbb{N}(\omega,\omega',|\omega \pm \omega'|) \times E(|\omega \pm \omega'|)E(\omega')/(\omega \pm \omega')^2 \omega'^2. \tag{2}$$

Redistribution of the energy involving triads of frequencies, as in Eq. (2), is characteristic of a dominant quadratic nonlinearity. Contribution of the cubic terms of Eq. (1) was found in [6] to vanish on the average, being of the next order of smallness. The form of Eq. (2) is in agreement with behavior expected from elementary theory of nonlinear oscillations (cf., for example, [7]). It corresponds to internal (frequency) resonance between the modes of the billiard, which effectively takes place when individual modes are not resolved, and hence a combination frequency of two source modes is indistinguishable from the frequency of another mode of the system. The resonance manifests itself in an early-time linear energy growth that can be linked to secular terms arising in regular perturbation theory [6].

Redistribution of the spectral energy in the billiard occurs due to nonlinear coupling of the modes. The average coupling strength is provided by the function [6]

$$\mathbb{N}(\omega_k,\omega_l,\omega_m) = (\pi/2)\langle N_{\underline{klm}} N_{\underline{klm}}\rangle = (\pi/2)\hat{N}_{\alpha\beta\gamma}\hat{N}_{\nu\mu\eta}K_{\alpha\nu}(\omega_k)K_{\beta\mu}(\omega_l)K_{\gamma\eta}(\omega_m). \tag{3}$$

Greek indices denote spatial degrees of freedom including both spatial position **x** and Cartesian indices, and repeated nonunderlined indices imply summation. The function $\mathbb{N}$ is symmetrical with respect to its arguments, rendering interaction strength of any triad of frequencies independent of energy transfer direction between them. Nevertheless, in typical classical-wave billiards with inverse modal spacing given by Weyl's series, $D \sim V_d \omega^{d-1} + \cdots$ [8], where V_d stands for d-dimensional volume of the billiard, the overall power input exhibits a net trend of the energy transfer toward regions of greater modal density, i.e., up the frequency spectrum.

Specifics of the physics of a particular system reside in statistics of its modes u_k and operator $\hat{N}$ that acts on them, $N_{klm} = \hat{N}_{\alpha\beta\gamma} u_k(\alpha) u_l(\beta) u_m(\gamma)$. Under the assumption that the modes are mutually uncorrelated Gaussian random vectors [9,10], the statistics are fully provided by the pairwise spatial modal correlator $K_{\alpha\beta}(\omega_k) = \langle u_{\underline{k}}(\alpha) u_{\underline{k}}(\beta) \rangle$. In the short-wavelength limit, when boundary effects are unimportant, the correlator can be approximated by means of the Green's function in unbounded medium, with long-range correlation being limited to billiard diameter L. Refined approximations of the correlator that include finite size and geometry effects can be constructed upon need, see [11] and references therein.

Under a random wave model (RWM), a mode inside a chaotic billiard can be viewed as superposition of constituent plane waves coming from all directions and having random amplitudes and phases [9]. In a multiwavespeed billiard, these waves can have different speeds of propagation and different amplitudes, requiring a modification to RWM [12]. Each pair of the constituent waves from the source modes interacts nonlinearly producing a constituent wave of the target mode. Two conservation laws must be obeyed in the process. The first requires frequency of the resultant wave to be equal either to the sum or difference of the source ones. A parallel can be drawn to energy conservation applied to particle scattering problems. The law is automatically satisfied by the internal-resonance structure of Eq. (2). The second law requires wave vectors of the constituent waves to sum, thus standing for conservation of wave pseudomomentum. In nondispersive systems interaction of constituent waves of the same wavespeed is always allowed by the above conservation laws, when the waves are collinear. This mechanism provides a nonzero background coupling strength for any frequency combination of source modes. Interaction of constituent waves of different wavespeeds, however, is only possible if the frequencies (and polarizations) of the source waves are in special relation to each other [13]. If the frequencies are such, this additional interaction channel is open, and nonlinear coupling strength is expected to be greater. Integral contribution of all constituent-wave interactions is provided by Eq. (3), statistics of the waves being incorporated by means of spatial correlator K. Precise conditions under which the maximum of the coupling strength is achieved depend on the specifics of the nonlinearity; for typical elastic solids they were seen to imply interaction of the constituent plane waves in a nearly collinear fashion [6]. By analogy to internal (frequency) resonance, a sharp increase in the coupling strength due to nonlinear interaction of constituent waves with different wave speeds is termed wave-vector resonance here.

To verify existence of the wave-vector resonance, a series of direct numerical simulations (DNS) was performed. An ensemble of discrete 2D square billiards with average boundary roughness of $1/24$ of the billiard size was taken; cf. [14]. Evolution of the wave-field inside the billiards was governed by first-order finite-difference version of the following two-wavespeed elastodynamic equation:

$$\ddot{u}_i = c_t^2 u_{i,jj} + (c_l^2 - c_t^2) u_{j,ij} + \varepsilon \Phi_{ijklmn} (u_{k,l} u_{m,n})_{,j}, \qquad (4)$$

where c_l and c_t are longitudinal and transverse wavespeeds, respectively. The nonlinear coupling term was chosen to be quadratic in derivatives of the displacements u, a form representative of the physical nonlinearity in isotropic elastic solids described by the five-constant theory [15]. The derivatives were coupled by the elementary isotropic tensor,

$$\Phi_{ijklmn} = \frac{1}{8}(\delta_{ik}\delta_{jm}\delta_{ln} + \delta_{ik}\delta_{jn}\delta_{lm} + \delta_{il}\delta_{jm}\delta_{kn} + \delta_{il}\delta_{jn}\delta_{km} + \delta_{im}\delta_{jk}\delta_{ln} + \delta_{im}\delta_{jl}\delta_{kn} + \delta_{in}\delta_{jk}\delta_{lm} + \delta_{in}\delta_{jl}\delta_{km}).$$

Strength of the nonlinearity was controlled by parameter ε, which was kept small on the order 10^{-2}, while $u = O(1)$. Dirichlet boundary conditions were imposed on the billiard boundaries. Initial displacement field was arranged so that only modes supporting two narrowband Gaussian peaks of the spectral energy centered at given frequencies ω_1 and ω_2 were excited. The width of the peaks was taken wide enough to encompass tens of modes. Evolution of the initial field up to one-tenth of the Heisenberg time, $t_H = 2\pi D = (A/2)(c_l^{-2} + c_t^{-2}) c_t / h$, where A is average billiard area, and h is finite-difference step length, was then computed by directly solving the governing ODEs (4). The procedure was performed for a number of realizations in order to obtain ensemble average of the spectral energy. Expected linear growth in time of the energy peaks centered at combinatoric frequencies, $\omega_{1\pm 2} = |\omega_1 \pm \omega_2|$, was observed. By varying central frequencies of the source peaks, and calculating average energy growth rate of the combinatoric peaks, the coupling strength (3) was recovered [6],

$$\mathbb{N}(\omega_{1\pm 2}, \omega_1, \omega_2) = (1/2) \dot{E}_{1\pm 2} \omega_1^2 \omega_2^2 / D(\omega_{1\pm 2}) E_1 E_2, \qquad (5)$$

where $E_{1,2}$ and $E_{1\pm 2}$ are total energies carried by the source and combinatoric peaks, respectively. Theoretical estimate of $\mathbb{N}$ was also obtained by means of Eq. (3) for the purpose of comparison with the DNS. A nonlinear operator containing specifics of the nonlinearity model was taken in accordance with the one used in Eq. (4),

$$\hat{N}_{\alpha=\{\mathbf{x},i\}\beta=\{\mathbf{x}',k\}\gamma=\{\mathbf{x}'',m\}} = \varepsilon \Phi_{ijklmn} \delta(\mathbf{x} - \mathbf{x}') \delta(\mathbf{x} - \mathbf{x}'') \partial^3 / \partial x_j \, \partial x_l' \, \partial x_n''.$$

Short-range behavior of the spatial modal correlator was approximated by its behavior in the unbounded medium,

$$K^{\infty}_{\alpha=\{\mathbf{x},i\}\beta=\{\mathbf{x}+\mathbf{r},j\}} = A^{-1}(c_l^{-2} + c_t^{-2})^{-1} \{ (\delta_{ij}/2)[c_l^{-2} J_0(k_l r) + c_t^{-2} J_0(k_t r)] + (\delta_{ij}/2 - \hat{r}_i \hat{r}_j)[c_l^{-2} J_2(k_l r) - c_t^{-2} J_2(k_t r)] \}. \qquad (6)$$

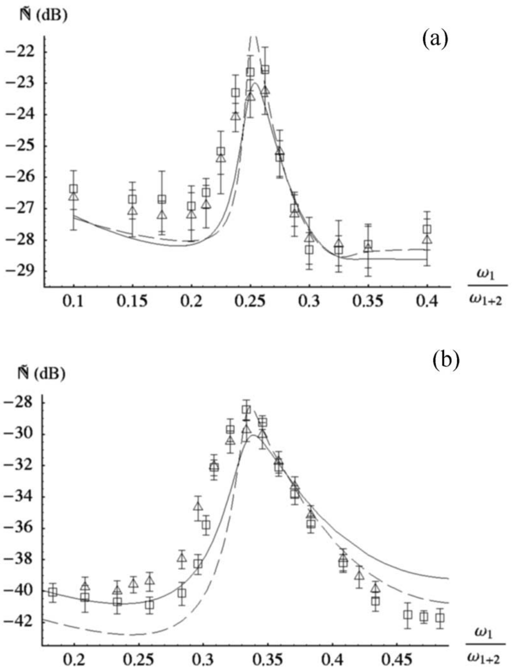

FIG. 1. Normalized coupling strength for (a) $c_l/c_t=2$, $\omega_{1+2}=1.2c_t/h$ and (b) $c_l/c_t=3$, $\omega_{1+2}=1.0c_t/h$. Solid and dash lines represent theoretical estimates, symbols △ and □ provide DNS data for nominal system sizes of 128 and 256 grid points, averaged over 25 and 10 realizations, respectively. Error bars correspond to one standard deviation.

The area of the billiard A enters the above expression due to normalization of the modes to unity.

The short-range correlator (6), as it is, leads to divergence of the spatial integrals at large separations in Eq. (3) due to slow asymptotic decay of Bessel functions. The divergence is a consequence of the quadratic form of the nonlinearity and problem dimensionality. It is not found in 3D, where the integrals converge [6]. To account for integration over the finite domain size and keep the integrals finite, long-range spatial correlation of the modes was restricted by billiard diameter L: $K=K^{\infty}\exp(-r/L)$ [16]. The restriction is qualitative and does not take into consideration specifics of the average domain shape. They could systematically be accounted for [11], but such undertaking lies beyond the scope of the present work. The normalized coupling strength was found to scale asymptotically as $\sqrt{L}$ with linear system size. This scaling is different from the case of 3D, where the strength remains $O(L^0)$ [6].

Comparison of the DNS results with theoretical estimates is given in Fig. 1. Energy growth rate at the sum frequency was utilized to obtain numerical values of the coupling strength; calculations at the difference frequency were carried out as well to check predicted symmetry of $\mathbb{N}$. To factor out dependence of the coupling strength on global parameters, and isolate behavior associated with frequency interrelation of the coupled modes, its normalized version was deemed best suited for analysis: $\tilde{\mathbb{N}}(\omega_1/\omega_{1+2},k_{1+2}L)=\pi^{-2}\varepsilon^{-2}A^2[1+(c_l/c_t)^{-2}]^3(k_1k_2k_{1+2})^{-4/3}\mathbb{N}$, with $k=\omega/c_t$. Plotted in this form, the coupling strength reveals the expected increase at the resonance frequency ratios in the vicinity of $\omega_1/\omega_{1+2}=(1\pm c_t/c_l)/2$. The ratios correspond to collinear interaction of two constituent transverse waves producing a longitudinal one. They define a lower and upper bound of the source to target frequency ratio of the coupled modes for which the wave vectors of the constituent waves can sum, i.e., their interaction is possible in accordance with pseudomomentum conservation law. Another constituent-wave interaction possible in physical solids, with $c_l/c_t>1$, involves a longitudinal and a transverse wave producing a longitudinal wave. Collinear wave-vector summation for this interaction type occurs at $\omega_1/\omega_{1+2}=[1\pm(3-c_l/c_t)/(1+c_l/c_t)]/2$. However, this resonance does not manifest itself for the given nonlinearity model. Under normal conditions its contribution to the coupling strength function is expected to be noticeably smaller than the one involving two transverse source waves due to equipartition of the energy carried by two different types of constituent waves inside a solid. Since most of the energy, in particular, a fraction $(c_l/c_t)^2>1$, is carried by transverse waves, their participation in the coupling is expected to be higher than that of longitudinal ones.

Although good qualitative agreement between theoretical estimates and DNS was found for parameters used, several remarks on their discrepancies ought to be made. A difference between background off-resonance coupling strength levels, especially at low frequency ratios, is noted. The difference can be attributed to the fact that though theoretical predictions based on Eq. (3) are fit-parameter free, some ambiguity in defining effective volume (2D area) of the billiard interior, where nonlinear mode coupling takes place, exists. In the present theoretical estimates it was taken exactly equal to the average domain area. No account of boundary and confinement effects was made by correlator form (6) with imposed qualitative long-range correlation dependence on the order of domain size. With nontrivial dependence of the coupling strength on the system size, however, specifics of the average domain shape may become important for quantitative agreement. Also, for system sizes within current DNS reach, the wavelength of the lowest source mode becomes large with respect to boundary roughness, and comparable to domain size at low-frequency ratios. Regular structure of the mode acquired in this case leads to deviation from the assumed modal statistics, and is expected to provide increased coherence of mode coupling in the interior of the billiard. Large-scale symmetry of the square billiard, however, seems to be of less significance in this case, as DNS calculations of the coupling strength for ensemble of rough-boundary 3:2 aspect-ratio quarter-stadium billiards produced compatible results.

As mentioned above, normalized coupling strength is predicted to asymptotically grow as $\sqrt{L}$ with system size. The prediction, however, is not supported by the current DNS data, see Fig. 2. The origins and implications of the disagreement are not fully understood at the time. However, it is speculated that it can be the result of frequency smoothing imposed on the coupling function by the finite width of the source energy distribution. The smoothing leads to the fact that only $\mathbb{N}$, averaged over characteristic peak width, could be recovered with the help of Eq. (5). Both decrease and broadening of the mode coupling resonance peak will follow

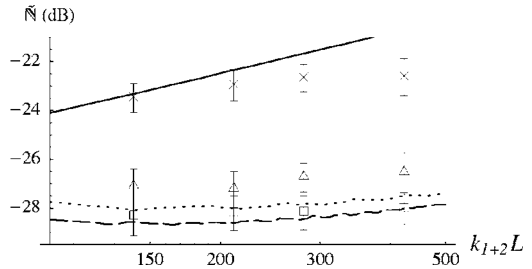

FIG. 2. Normalized coupling strength for $c_l/c_t=2$, $\omega_{1+2}=1.2c_t/h$. Dot, solid, and dash lines represent theoretical estimates at $\omega_1/\omega_{1+2}=0.15$, 0.25, and 0.35. Symbols △, ×, and □ provide DNS data for nominal system sizes of 128, 192, 256, and 384 grid points, averaged over 25, 25, 10, and 10 realizations, respectively.

from this smoothing. System sizes currently available for DNS realizations do not allow direct observation of the expected $\sqrt{L}$ scaling, or a conclusive statement regarding its absence. Decrease of the source energy distribution width would be problematic, in that it needs to contain many modes in order for the statistical approach to be valid.

In summary, the existence of the wave-vector resonance in the mode coupling strength, responsible for nonlinear redistribution of the average spectral energy, was verified by direct numerical simulation in a two-wavespeed chaotic billiard with nonlinearity representative of isotropic elastic solids. Qualitative agreement with theoretical estimates in the absence of fit parameters was observed. The location of the coupling strength peak was found to correspond to collinear interaction of constituent waves of different wavespeeds. The location was determined from arguments based on conservation principles, and to leading order depends solely on linear system quantities.

This work was supported in part by the National Science Foundation Grant No. CMS-0201346.

[1] S. E. Skipetrov and R. Maynard, in *Wave Scattering in Complex Media*, edited by B. A. van Tiggelen and S. E. Skipetrov (Kluwer Academic Publishers, Dordrecht, 2003).
[2] R. Bressoux and R. Maynard, in *Waves and Imaging through Complex Media*, edited by P. Sebbah (Kluwer Academic Publishers, Dordrecht, 2001); T. Wellens, B. Grémaud, D. Delande, and C. Miniatura, Phys. Rev. E **71**, 055603(R) (2005).
[3] S. E. Skipetrov, J. Opt. Soc. Am. B **21**, 168 (2004).
[4] B. Liu, A. Yamilov, Y. Ling, J. Y. Xu, and H. Cao, Phys. Rev. Lett. **91**, 063903 (2003).
[5] R. L. Weaver, in *Waves and Imaging through Complex Media*, edited by P. Sebbah (Kluwer Academic Publishers, Dordrecht, 2001).
[6] A. Akolzin and R. L. Weaver, Phys. Rev. E **69**, 066605 (2004).
[7] L. Mierovitch, *Elements of Vibration Analysis* (McGraw-Hill, New York, 1986), Chap. 10.
[8] M. C. Gutzwiller, *Chaos in Classical and Quantum Mechanics* (Springer-Verlag, New York, 1990), Sec. 16.2.
[9] M. V. Berry, J. Phys. A **10**, 2083 (1977); P. O'Connor, J. Gehlen, and E. J. Heller, Phys. Rev. Lett. **58**, 1296 (1987).
[10] S. W. McDonald and A. N. Kaufman, Phys. Rev. A **37**, 3067 (1988).
[11] F. Toscano and C. H. Lewenkopf, Phys. Rev. E **65**, 036201 (2002); J. D. Urbina and K. Richter, *ibid.* **70**, 015201(R) (2004).
[12] K. Schaadt, T. Guhr, C. Ellegaard, and M. Oxborrow, Phys. Rev. E **68**, 036205 (2003); A. Akolzin and R. L. Weaver, *ibid.* **70**, 046212 (2004).
[13] G. L. Jones and D. R. Kobett, J. Acoust. Soc. Am. **35**, 5 (1963).
[14] R. L. Weaver and J. Burkhardt, J. Acoust. Soc. Am. **95**, 3186 (1994); R. L. Weaver and O. I. Lobkis, J. Sound Vib. **231**, 1111 (2000).
[15] R. W. Ogden, *Nonlinear Elastic Deformations* (Ellis Horwood Ltd., Chichester, 1984), Sec. 6.1.6.
[16] Terms associated with spatial derivatives of the long-range correlation factor are neglected in calculation of $\mathbb{N}$ (3), as being $(kL)^{-1}$ smaller than the similar terms associated with the short-range part (6) of the full correlator K.